Journal of Electroanalytical Chemistry 636 (2009) 123–127

Contents lists available at ScienceDirect

Journal of Electroanalytical Chemistry

journal homepage: www.elsevier.com/locate/jelechem

Short Communication

Glucose sensing by electrochemically grown copper nanobelt electrode

Ting-Kai Huang [a], Kuan-Wen Lin [a], Sze-Ping Tung [a], Ta-Ming Cheng [a], I-Chun Chang [a], You-Zung Hsieh [a], Chi-Young Lee [b], Hsin-Tien Chiu [a,*]

[a] Department of Applied Chemistry, National Chiao Tung University, Hsinchu 30050, Taiwan, ROC
[b] Center for Nanotechnology, Materials Science and Microsystems, National Tsing Hua University, Hsinchu, 30043 Taiwan, ROC

ARTICLE INFO

Article history:
Received 16 January 2009
Received in revised form 13 August 2009
Accepted 28 August 2009
Available online 1 September 2009

Keywords:
Copper nanobelt
Electrochemical deposition
Glucose sensing

ABSTRACT

A simple design of growing Cu nanobelt (NB) electrode for glucose sensing is presented. Cu NBs were grown directly on carbon electrodes by using electrochemical deposition. The average width, thickness and length of the NBs were about 50 nm, 20 nm and several tens of micrometers, respectively. Cyclic voltammetric (CV) experiments showed that a Cu NB electrode grown by a reduction charge of 0.5 C on a substrate of 0.018 cm^2 enhanced glucose oxidation ability. For glucose sensing, the electrode exhibited a high sensitivity of 79.8 μA/mM and a measurable detection limit of 10 μM in amperometric detection.

1. Introduction

Development of cheap, reliable, and fast sensors for glucose detection is important because it involved in many areas, including food industry, clinic diagnostics, and biotechnology. Commercial pocket-sized blood sugar sensors are the examples. Based on glucose oxidase electrodes, these sensors have benefited diabetic patients for conveniently monitoring their blood sugar levels at any time [1–7]. However, to fabricate these electrodes, complicated immobilization processes are needed. In addition, they suffer from intrinsic instabilities and are sensitive to oxygen concentration in the environment. On the other hand, there are more and more attempts to develop non-enzymatic sensors constructed from nanostructured materials with increased surface areas recently. These sensors, containing electrodes with high electroactive surfaces, can enhance current responses significantly. In many cases, sensing selectivity of glucose relative to interfering species L-ascorbic acid and uric acid can be increased as well [8–10]. Sensors constructed from nanostructured Pt, Au, Si, carbon nanotube (CNT), CNT/metal composite and CuO electrodes are known examples [8–22]. Among them, electrodes composed of Cu-based nanostructures have been reported for potential developments [17–22]. The Cu-based electrodes do contain some disadvantages. They are non-selective towards other carbohydrates, such as fructose and sucrose, and need to be operated in an alkaline media. Despite of these, they displayed high sensitivities and low detection limits for glucose sensing [21,22]. In addition, Cu is relatively low cost so electrodes may be mass produced for applications which require disposable sensing elements. Recently, fabrication of Cu nanobelts (NBs) via a Galvanic reduction process has been achieved [23]. Inspired by previous works of employing Cu-based electrodes for glucose sensing [21,22], we anticipate that the Cu NB, with its thin native oxide layer on the highly exposed surface, may be employed as an alternative electrode material. Here, we report our exploration of a simple electrochemical deposition process to grow Cu NBs on carbon screen printed electrodes (SPE) for glucose sensing. Our discoveries are discussed below.

2. Experimental

2.1. Electrolyte preparation

$CuCl_2$ (0.034 g, 0.25 mmol) was added to a stirring aqueous solution (100 mL) of cetyltrimethylammonium chloride (CTAC, 0.9 mM) and HNO_3 (2.5 mM) in a glass vial. Immediately, the mixture turned light blue. After a portion of the solution (10 mL) was transferred to another glass vial, it was placed in a water bath controlled at 290 K.

2.2. Electrochemical fabrication of Cu electrodes

In a two-electrode electrochemical cell composed of a DC power supply and two carbon electrodes, Cu NBs were grown on the cathode, which was a carbon SPE purchased from Zensor R&D with a geometric area of 0.018 cm^2. The anode was fabricated by painting carbon paste uniformly on transparent projection slides followed by drying them on a hotplate at 353 K for 3 h under air. They were

* Corresponding author. Tel.: +886 3 5131514; fax: +886 3 5723764.
E-mail address: htchiu@faculty.nctu.edu.tw (H.-T. Chiu).

0022-0728/$ - see front matter © 2009 Elsevier B.V. All rights reserved.
doi:10.1016/j.jelechem.2009.08.011

cleaned with deionized water before use. After the cathode and the anode were immersed in the electrolyte for 3 min, a fixed DC voltage of 2.0 V was supplied across the electrodes. At 290 K without stirring, the cathode surface turned into a copper-like color gradually. After 24 h, a total charge of ca. 0.5 C was supplied. The cathode was removed and rinsed with deionized water. To avoid oxidation, the as-prepared Cu NB electrodes were stored in a N_2 filled glove box to prevent excessive surface oxidation. For comparison of electrochemical properties, Cu nanoparticle (NP) and Cu foil electrodes were also fabricated. Cu NPs were electrochemically grown on SPE using the same reduction charge of 0.5 C [24]. Cu foils (Aldrich), with exposed geometric area of 0.018 cm^2, were prepared by covering their surfaces with properly sized Scotch tapes (3 M).

2.3. Instruments

The electrodes were characterized by the following instruments: scanning electron microscope (SEM, JEOL JSM-6330F at 15 kV), energy dispersive spectrometer (EDS, Oxford Link Pentafet), transmission electron microscope (TEM, JEOL JEM-2010F at 200 kV and JEOL JEM-4000EX), and X-ray diffractometer, (XRD, Bruker AXS D8 Advance). Cyclic voltammetric (CV) and chronoamperometric experiments were carried out using a CHI 802 electrochemical workstation (CH Instruments, Austin, TX, USA). Amperometric curve of the electrodes was recorded at 0.6 V in a stirring 50 mM NaOH solution in air.

3. Results and discussion

3.1. SEM characterization of Cu nanobelts and nanoparticles grown on electrodes

Fig. 1 shows the SEM images of the as-prepared Cu NBs and NPs electrodes. As displayed in Fig. 1A, one-dimensional (1-D) nanostructures, several tens of μm in length, grow densely to cover the entire carbon electrode surface. The EDS (Fig. S1A) confirmed that the product was composed of Cu mainly. The inset in Fig. 1A shows clearly a bending belt with a thickness of 20 nm. A width distribution histogram of one hundred NBs provided an average width of 46 nm and a main distribution range of 35–55 nm (Fig. S1B). The belt width can be adjusted by varying the reaction mixture concentration and the applied potential. For example, when all ingredients in the mixture was doubled, the NBs displayed increased width (average: 185 nm, main distribution: 120–240 nm) and zigzag edges (Figs. S1C–D). The diameters of the Cu NP aggregates shown in Fig. 1B is in the range of 100–300 nm.

3.2. TEM characterization of Cu nanobelts

In Fig. 2A, the TEM image of a single NB lying flatly is shown. Dark lines from internal stresses, typical for NB materials, are clearly observed [23,25–33]. The selected area electron diffraction (SAED, inset) displays a set of dots with a hexagonal symmetry, exemplified by three spots marked with triangles. This indicates that the NB was single-crystalline. From the pattern, the crystallographic zone axis can be indexed to be Cu [1 1 1]. The brightest set of spots is assigned to Cu {2 2 0} reflections (JCPDF 89–2838) with a *d*-spacing of 0.128 nm. It also indicates that the NB's basal plane was {1 1 1}. Growth direction of the NB is determined to be along [−1 1 0] direction as concluded from the SAED pattern. Fig. 2B presents a high resolution TEM (HRTEM) image from the marked region in Fig. 2A. Two {2 2 0} lattice planes are identified on the basis of their dihedral angle of 120°. This is consistent with the theoretical value of an fcc structure. The *d*-spacing is measured to be 0.128 nm, close to the literature value of Cu, 0.1278 nm (JCPDF 89–2838). These HRTEM characterizations agree with the SAED result. X-ray diffraction (XRD) patterns also confirmed that the NBs had an fcc structure (Fig. S2). The estimated lattice parameter *a*, 0.36 nm, is consistent with the reported value of Cu, 0.362 nm (JCPDF 89–2838). In the SAED in Fig. 2A, in addition to the pattern of Cu, there is another set of dimmer hexagonal spots, exemplified by the one marked with a white square. This suggests the presence of another cubic phase material with a *d*-spacing of 0.25 nm. This is close to the {1 1 1} spacing value of Cu_2O, 0.246 nm (JCPDF 78–2076). Since the reflections from Cu_2O are not observed in the XRD pattern (Fig. S2), we conclude that the quantity of Cu_2O in the sample is little. Origin of Cu_2O is proposed to be from oxidation of the NB surface in an ambient environment.

3.3. Cyclic voltammograms of Cu electrodes

Fig. 3 shows the CV (scan rate = 50 mV/s) behaviors of the Cu NB, NP and foil electrodes in a phosphate buffer solution (PBS, pH = 7.4). For the NB electrode, it shows significantly higher reduction/oxidation responses than the other two do. This indicates that the NB electrode has a relatively large electrochemical surface area [24]. The oxidation peaks at −0.02, 0.18 and 0.32 V are referred to

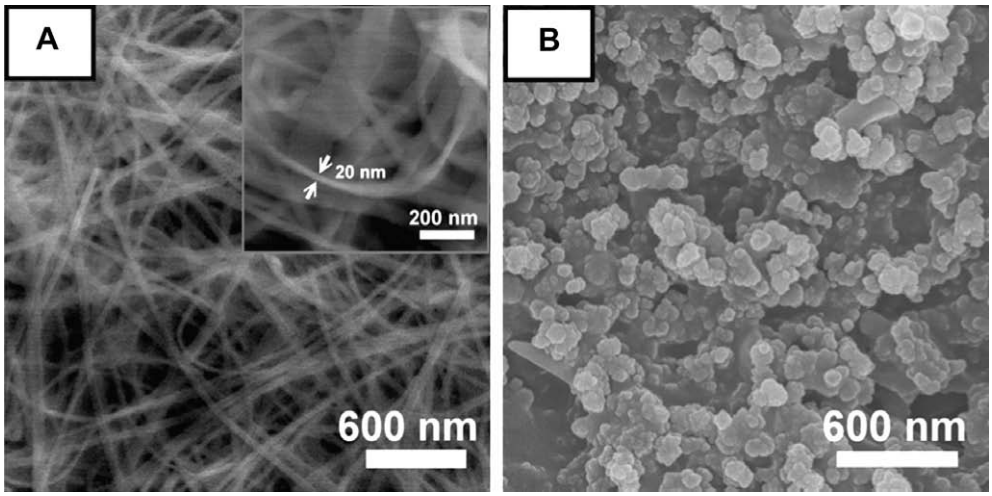

Fig. 1. SEM images of (A) Cu NBs (inset: enlarged view showing bending and thickness of NBs) and (B) NPs grown on carbon electrodes.

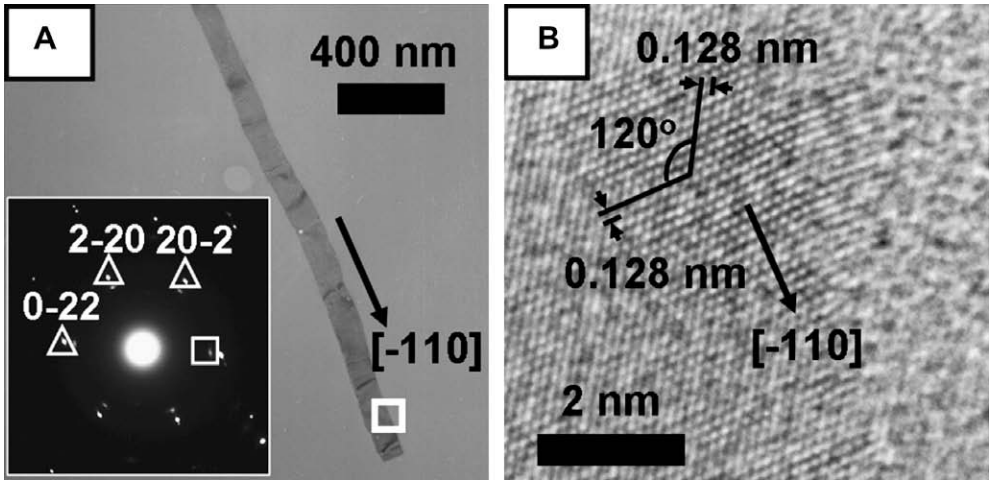

Fig. 2. (A) TEM image and SAED pattern (inset) from the white square of an individual Cu NB. (B) HRTEM image from the white square in (A).

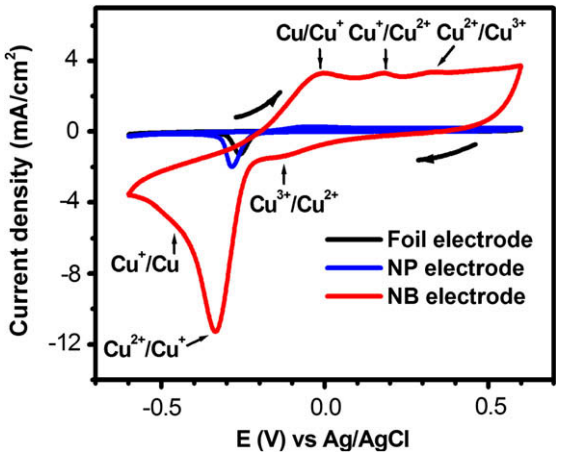

Fig. 3. CVs of Cu foil (black), NP (blue) and NB (red) electrodes. (For interpretation of the references to colour in this figure legend, the reader is referred to the web version of this article.)

the conversion of Cu(0)–Cu(I), Cu(I)–Cu(II) and Cu(II)–Cu(III) [18]. In the reduction cycle, the peak at −0.33 V and the shoulder at −0.46 V correspond to the translations of Cu(II)–Cu(I) and Cu(I)–Cu(0), respectively [24]. The other weak wave at −0.14 V is assigned to the conversion of Cu(III)–Cu(II). It is surprising that the reductive peak intensity of the NP electrode is only one seventh of that of the NB electrode. This suggests that the aggregated NPs could not expose their surfaces as efficiently as the NBs.

3.4. Amperometric sensing of glucose

To compare electrocatalysis of glucose oxidation by the nanostructured Cu electrodes, CV studies of both NB and NP electrodes were performed. As shown in Fig. 4A, in a blank alkaline solution (50 mM $NaOH_{(aq)}$), clear current increases corresponding to a Cu(II)/Cu(III) redox couple are observed above 0.7 and 0.75 V for the NB and the NP electrodes, respectively [17]. For both electrodes in 0.1 M glucose mixed with 50 mM $NaOH_{(aq)}$, additional waves, corresponding to irreversible glucose oxidation, appear. The oxidation is attributed to a Cu surface oxide assisted electrocatalytic process, as described in previous reports [17,18,21,22]. For the Cu NB electrode, dramatic enhancement of the oxidation current can be observed between 0.2 and 0.7 V. For the NP electrode, the oxidation current increase starts only at 0.4 V. Fig. 4B illustrates amperometric measurements of glucose by the nanostructured Cu electrodes (0.6 V in aerated 50 mM $NaOH_{(aq)}$). The NB electrode provides a much higher current response than the NP electrode does, as demonstrated in Fig. 4C. The inset in Fig. 4B shows that the NB electrode can offer sensitive and stable detection in μM concentrations. A sensitivity of 79.8 μA/mM with a linear dependence (R^2 value, 0.998) of oxidation current to glucose concentration (10.0 μM–1.13 mM) is observed for the NB electrode. The minimum detectable concentration shown in Fig. 4B and C is 10 μM. These results were reproducible in several experiments. We anticipate the performance may be improved further upon additional electrode developments. For example, a minimum measurable concentration of 0.5 μM was observed (Fig. S5). For comparison, the NP electrode shows a lower sensitivity of 6.2 μA/mM. This probably is due to aggregation of the NPs during their growth on the electrode surface. Performances of various nanostructured non-enzymatic electrodes reported previously are summarized in Table 1. Among these, the CuO nanowire (NW) electrode reported by Zhuang et al. showed the highest sensitivity and the lowest detection limit [22]. The CuO nanorod (NR) electrode reported by Batchelor-MacAuley et al. performed well too [21]. Since geometric areas of the electrodes shown in Table 1 varied widely, quantitative comparisons are difficult. The sensitivity and the detection limit of our Cu NB electrode were inferior to those two mentioned above. Considering the small geometric area, 0.018 cm^2, of the Cu NB electrode fabricated in this study, we feel that its performance is comparable to the other literature examples shown in Table 1. The performance of our electrode could be enhanced further by adjusting the amount of Cu NBs deposited, the geometric area employed, and the extent of oxide layer grown.

In real physiological samples, interfering species such as chloride ion, L-ascorbic acid (AA) and uric acid (UA) normally co-exist with glucose. The concentration of chloride ion is about ten times of that of glucose level. The AA and UA concentrations are about one-tenth of the glucose value. Amperometric responses of the NB electrode towards the addition of these species (Cl^-: 1 mM, AA and UA: 10 μM) followed by glucose (100 μM successively) were examined. As shown in Fig. 4D, AA and UA do not produce significant responses while the glucose response remains at about 60% of the value in the presence of 1 mM chloride ion shown in Fig. 4B. On the other hand, the Cu NB electrodes demonstrated their abilities to electro-oxidize other carbohydrates, such as fructose and sucrose, in CV studies. However, similar to the cases reported before, they did not display special selectivity among the carbohydrates. This is a common challenge yet to be solved for non-enzymatic electrodes [17,19–21].

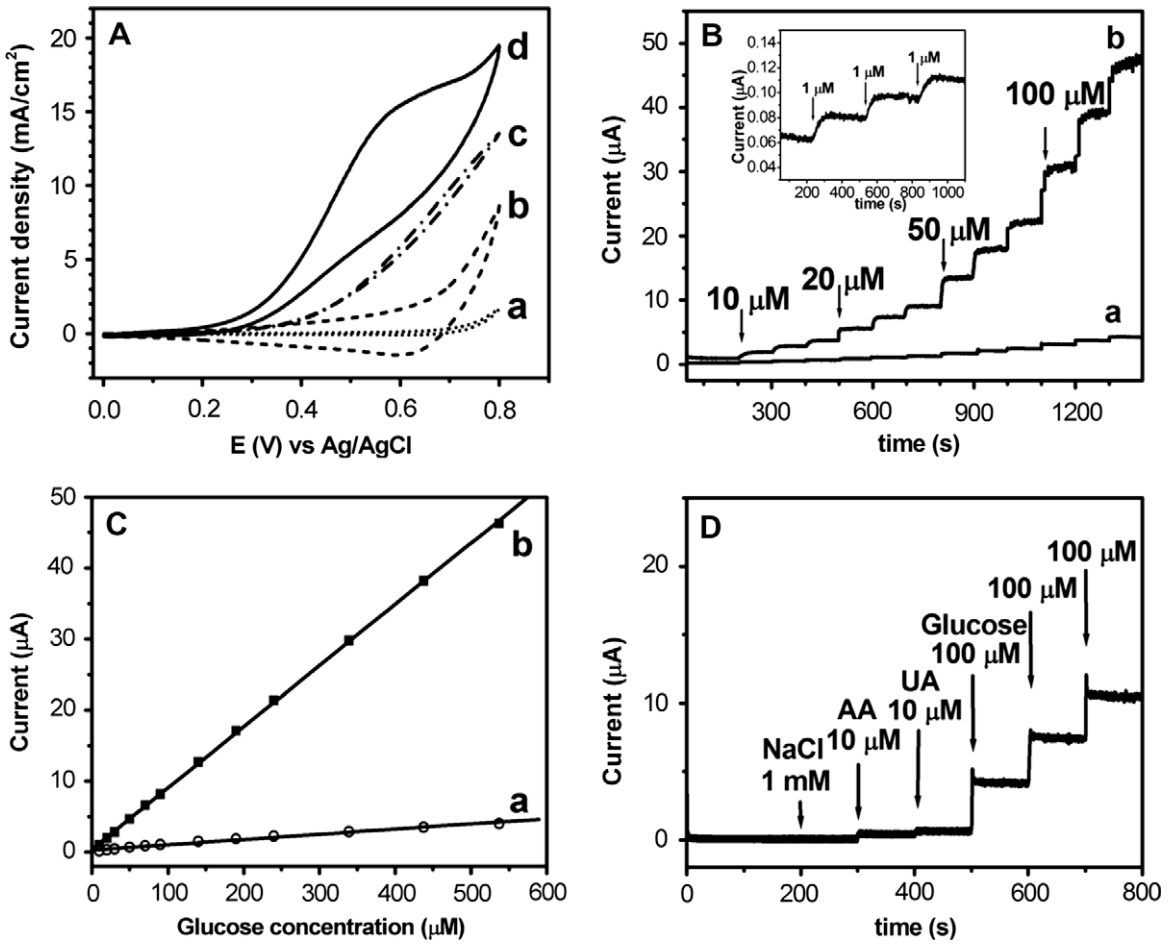

Fig. 4. Electrochemical data of Cu electrodes in 50 mM NaOH at 50 mV/s. (A) CV diagrams of (a) NP and (b) NB electrodes without glucose, and (c) NP and (d) NB electrodes in 0.1 M glucose; (B) Amperometric responses of (a) NP and (b) NB electrodes to successive additions of glucose (inset: successive additions of 1 μM glucose); (C) Current responses of (a) NP and (b) NB electrodes to glucose concentrations from the data in (B); (D) Amperometric responses (at 0.6 V) of a NB electrode to interferences from chloride ion (1 mM), ascorbic acid (AA, 10 μM) and uric acid (UA, 10 μM) prior to successive additions of glucose.

Table 1
Comparison of various non-enzymatic glucose sensors.

Electrode	Geometric area (cm^2)	Sensitivity ($\mu A\ mM^{-1}$)	Detection limit (μM)	Reference
Cu NBs	0.018	79.8	10	This study
CuO NR bundles	N/A	450	1.2[b]	[21]
CuO NW bundles	0.2	490	0.049[b]	[22]
Cu NPs/MWCNT	0.07	17.76	0.21[b]	[17]
Cu particles	0.031	111.6	0.7[b]	[18]
DMG functionalized Cu NPs	0.07	49	0.5[b]	[19]
Cu NPs/SWCNT/ Nafion	0.07	256	0.25[b]	[20]
Pt NTs	0.1256	0.1[a]	1.0[b]	[9]
Mesoporous Pt	0.02	9.6[a]	N/A	[10]
Macroporous Pt	0.292	31.3[a]	0.1[b]	[11]
Pt–Pd NPs/ MWCNT	0.09	17.8[a]	1.8[b]	[12]
MWCNT	N/A	4.36[a]	N/A	[8]
Au NPs	0.02	179[a]	0.05[c]	[13]
Porous Au	0.33	32[a]	2[b]	[14]
Macroporous Au	0.5	11.8[a]	5[b]	[15]

[**] MWCNT – multi-walled CNT; DMG – dimethylglycoxime; SWCNT – single-walled CNT; NTs – nanotubes; N/A – not available.
[a] Estimated from three times of the standard deviation of the blank signal.
[b] The unit is $\mu A\ cm^{-2}\ mM^{-1}$.
[c] The minimum concentration could be detected.

4. Conclusions

In conclusion, we have demonstrated a simple low-cost electrochemical deposition process to grow Cu NBs on carbon screen printed electrodes for glucose sensing. Our results indicate that the Cu NB electrode can enhance electrocatalytic ability of glucose oxidation significantly. The high performance may be attributed to the large electrochemical surface area of the NBs and the highly ordered belt surface planes [34]. Presence of better contacts between the NBs and the substrate may also show positive effects. Thus, the kinetically-controlled electrooxidation of glucose is amplified and the response current is increased. We anticipate that upon further development, these Cu NB electrodes will perform exceptionally in glucose sensing applications.

Acknowledgments

This work is supported by the National Science Council and "Aim for the Top University Plan" of the National Chiao Tung University and the Ministry of Education of Taiwan, the Republic of China.

Appendix A. Supplementary material

Supplementary data associated with this article can be found, in the online version, at doi:10.1016/j.jelechem.2009.08.011.

References

[1] See World Health Organization (WHO), <http://www.who.int/en/>.
[2] L.C. Clark, C. Lyons, Ann. NY Acad. Sci. 102 (1962) 29.
[3] H.T. Zhao, H.X. Ju, Anal. Biochem. 350 (2006) 138.
[4] S. Hrapovic, Y. Liu, K.B. Male, J.H.T. Luong, Anal. Chem. 76 (2004) 1083.
[5] E.S. Forzani, H.Q. Zhang, L.A. Nagahara, I. Amlani, R. Tsui, N.J. Tao, Nano Lett. 4 (2004) 1785.
[6] X. Wen, Y.T. Xie, M. Wing, C. Mak, K.Y. Cheung, X.Y. Li, R. Renneberg, S. Yang, Langmuir 22 (2006) 4836.
[7] H. Lee, S.W. Yoon, E.J. Kim, J. Park, Nano Lett. 7 (2007) 778.
[8] S.J. Ye, Y. Wen, W.D. Zhang, L.M. Gan, G.Q. Xu, F.S. Sheu, Electrochem. Commun. 6 (2004) 66.
[9] J.H. Yuan, K. Wang, X.H. Xia, Adv. Funct. Mater. 15 (2005) 803.
[10] S. Park, T.D. Chung, H.C. Kim, Anal. Chem. 75 (2003) 3046.
[11] Y.Y. Song, D. Zhang, W. Gao, X.H. Xia, Chem. Eur. J. 11 (2005) 2177.
[12] H.-F. Cui, J.-S. Ye, W.-D. Zhang, C.-M. Li, J.H.T. Luong, F.-S. Sheu, Anal. Chim. Acta 594 (2007) 175.
[13] K.B. Jena, C.R. Raj, Chem. Eur. J. 12 (2006) 2702.
[14] S. Cho, C. Kang, Electroanalysis 19 (2007) 2315.
[15] Y. Li, Y.-Y. Song, C. Yang, X.-H. Xia, Electrochem. Comm. 9 (2007) 981.
[16] G. Wang, K. Mantey, M.H. Nayfeh, S.-T. Yau, Appl. Phys. Lett. 89 (2006) 243901.
[17] X. Kang, Z. Mai, X.-Y. Zou, P.-X. Cai, J.-Y. Mo, Anal. Biochem. 363 (2007) 143.
[18] J. Zhao, F. Wang, J. Yu, S. Hu, Talanta 70 (2006) 449.
[19] Q. Xu, Y. Zhao, J.-Z. Xu, J.-J. Zhu, Sens. Actuators B: Chem. 114 (2006) 379.
[20] K.B. Male, S. Hrapovic, Y. Liu, D. Wang, J.H.T. Luong, Analy. Chim. Acta 516 (2004) 35.
[21] C. Batchelor-McAuley, Y. Du, G.G. Wildgoosea, R.G. Compton, Sens. Actuators B: Chem. 135 (2008) 230.
[22] Z.J. Zhuang, X.D. Su, H.Y. Yuan, Q. Sun, D. Xiao, M.M.F. Choi, Analyst 133 (2008) 126.
[23] T.-K. Huang, T.-H. Cheng, M.-Y. Yen, W.-H. Hsiao, L.-S. Wang, F.-R. Chen, J.-J. Kai, C.-Y. Lee, H.-T. Chiu, Langmuir 23 (2007) 5722.
[24] J.-M. Zen, C.-T. Hsu, A.-S. Kumar, H.-J. Lyuu, K.-Y. Lin, Analyst 129 (2004) 841.
[25] J. Bai, Y. Qin, C. Jiang, L. Qi, L. Chem. Mater. 19 (2007) 3367.
[26] Y. Sun, B. Mayers, Y.-N. Xia, Nano Lett. 3 (2003) 675.
[27] J.L. Zhang, J.M. Du, B.X. Han, Z.M. Liu, T. Jiang, Z.F. Zhang, Angew. Chem. Int. Ed. 45 (2006) 1116.
[28] N. Zhao, Y. Wei, N. Sun, Q. Chen, J. Bai, L. Zhou, Y. Qin, M. Li, L. Qi, Langmuir 24 (2008) 991.
[29] J. Zhang, H. Liu, Z. Wang, N. Ming, Appl. Phys. Lett. 91 (2007) 133112.
[30] Y. Chen, S. Milenkovic, A.W. Hassel, Nano Lett. 8 (2008) 737.
[31] Z. Liu, S. Li, Y. Yang, S. Peng, Z. Hu, Y. Qian, Adv. Mater. 15 (2003) 1946.
[32] Z.L. Wang, Adv. Mater. 15 (2003) 432.
[33] Z.W. Pan, Z.R. Dai, Z.L. Wang, Science 291 (2001) 1947.
[34] I. Takahashi, O. Koga, N. Hoshi, Y. Hori, J. Electroanal. Chem. 533 (2002) 135.